An Efficient Method for Kidney Segmentation on Abdominal CT Images

Daw-Tung Lin[1], Chung-Chih Lei[1], and Shiao-Yun Hsiung[2]
1. Department of Computer Science, Chung-Hua University, Hsin Chu, Taiwan
2. Radiology Department, Taichung Veterans General Hospital, Taichung, Taiwan

Abstract

This paper describes an effective method for kidney segmentation on abdominal CT images. This segmentation system is expected to assist the physicians on clinical diagnosis and educational training. The proposed method is partitioned into two processes. First, the ROI is extracted using the statistics of geometric location of kidney on the abdomen area. In addition, the noise is removed by applying the conditional median filter and performing the primary pixel aggregation. In the following stage, the kidney is identified by the proposed operations including adaptive region-growing, efficient filling operation, labeling, and mathematical morphology operation. Furthermore, in order to show different view for physicians, we have implemented a visualization tool to show the renal segmentation contour automatically.

1 Introduction

Image segmentation is one of the most popular topics for computer aided medical image analysis and diagnosis such as segmentation of liver, lung, kidney, and so on. Generally speaking, there are two main reasons for the need of computer aided segmentation: to improve user-guided segmentation [12], and to acquire segmentation prior to visualization or quantification [2]. In the recent years, many computer- aided diagnostic (CAD) systems have been developed to assist physicians to diagnose symptoms in the fields of lung cancer, brain tumor and breast diseases diagnosis. However, there are less literatures and researchers on the kidney segmentation. This is because that understanding the various aspects of kidney by using computer technologies is difficult.

There were three categories methods for kidney segmentation: region-based, knowledge-based and snake-based approaches. Pohle and Toennies[2][3][4] developed a region growing algorithm that learns its homogeneity criterion automatically from characteristics of the region to be segmented. Wang, et. al.[5] proposed a constrained optimization approach in which region information can be computed as extra constraints within the contour energy minimization framework. Kobashi and Shapiro [6] described a knowledge-based procedure for identifying and extracting organs from normal CT imagery. Based on the above consequences, we attempt to combine the advantages of the above-mentioned works and develop a more promising method for kidney segmentation on abdominal CT images, and then exhibit the exploited system for the ease of kidney observation. The rest of this article is organized as following: the pre-processing is illustrated in Section 2, the detailed methodology of kidney segmentation is stated in Section 3, the experimental results and conclusion are mentioned in Sections 4 and 5, respectively.

2 Pre-processing and ROI Extraction

In this section, we will describe the pre-processing approach for the ROIs extraction for left and right kidney. In order to simplify the question of different slice thickness of CT images and machine setting resulted from various hospitals and patients, we start to proceed from the i_{th} slice which is approximately in the middle of the sequence where $i = \lfloor \frac{n}{2} \rfloor$, and n is the total number of slices of one patient case. The middle slice shows the obvious kidney image, and easy to review for each datasets. The spine is one important landmark in our work, which is used to allocate the reference position of kidney. The spine (denoted as "**X**" in Fig. 1) is approximately located at the position

∗ This work was supported in part by the National Science Council, Taiwan, R.O.C. (NSC91-2213-E-216-007). Acknowledgement also due to Dr. Bai-Lu Shih at the Radiology Department, Chungli Li-Shin Hospital, for invaluable discussions and suggestions.

∗ Corresponding author: Daw-Tung Lin, Department of Computer Science and Information Engineering, Chung-Hua University, 30 Tung Shiang, Hsin Chu, Taiwan 30067 (email:dalton@chu.edu.tw).

(0.5 l_1 ,0.56 l_2) where l_1 is the length of horizontal axis and l_2 is the length of vertical axis of the abdominal boundary. The abdominal boundary is obtained by the following algorithm:

For all pixels f(i,j) in the CT image

Do

For each direction (f(i±7, j), f(i,j±3))

if the total number of nonzero pixels on that direction is less than 1

then set f(i, j) = 0

The initial ROI of left kidney is then located by the following rules: 1. the distance between spine and the right boundary of ellipse is 25 pixels; 2. the distance between the upper boundary of ellipse and the border of abdominal boundary is 22 pixels; 3. the distance between the lower boundary of ellipse and the border of abdominal boundary is 25 pixels; 4. the distance between the left boundary of ellipse and the abdominal boundary is 45 pixels. The ROI of right kidney can be determined in the same way. Therefore, the initial ROI ellipse center X_0, Y_0 can be decided. Both of the kidneys usually appear in the range of a specific inclined angle. To obtain more meaningful ROIs, we rotate the preliminary ROIs and represent the new result in Equation (1).

$$\begin{pmatrix} X' \\ Y' \end{pmatrix} = \begin{pmatrix} \cos\theta & -\sin\theta \\ \sin\theta & \cos\theta \end{pmatrix} \begin{pmatrix} X - X_0 \\ Y - Y_0 \end{pmatrix} + \begin{pmatrix} X_0 \\ Y_0 \end{pmatrix} \qquad (1)$$

where (X',Y') denotes the final coordinates of the center of ROI ellipse, (X_0,Y_0) is the coordinate of the center of the initial ROI, θ =60 ^{0}. The relationship between (X',Y') and (*X, Y*) can be obtained by geometric transformation of translation and rotation. Consequently, the ROIs of the left and the right kidney can be found and located as plotted in dotted line in Fig. 1. One of the results of ROI extraction is shown in Fig. 2. This transformation possesses high flexibility for positioning a large variety of objects. The ROIs include two parts which are true kidney region and non-kidney region such as liver, spleen, fat and so on. To eliminate the preliminary noises, we applied the smooth filtering operation as shown

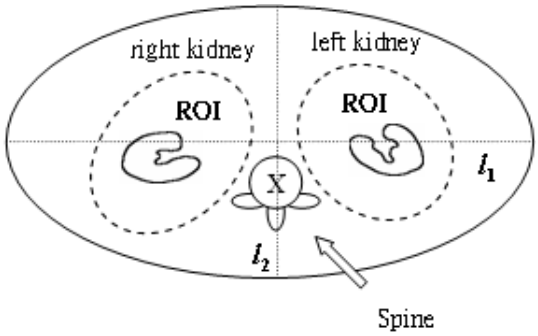

Figure 1: ROIs are plotted in dotted lines.

in Equation 2:

$$\mu_{left\_ROI} = \frac{\sum\sum f_{left\_ROI}(i,j)}{n_{left\_ROI}} \qquad (2)$$

where $f_{left\_ROI}(i,j)$ denotes the intensity of pixel (*i, j*) and n_{left_ROI} shows the number of pixels on the left ROI, μ_{right_ROI} is the filtering operation for the right ROI. It seems trivial and ordinary, but still contributes to facilitate the follow-up process. In addition, the mean values μ_{left_ROI}, μ_{right_ROI} just need to be calculated once for the entire dataset, because the rest of slices remain approximately equal intensity distribution on kidney images for one patient [8].

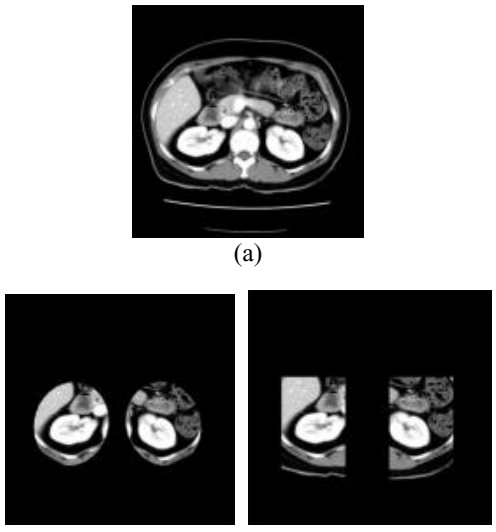

(a) (b) (c)

Figure 2: (a) Original image, (b) ROIs image extracted by the proposed technique, and (c) ROIs image obtained by Tsagaan[1].

The median filter [11] is particularly effective for the noise pattern consisting of strong spikelike components. The gray level of each pixel is replaced by the median of the gray levels in its neighborhood, instead of using the average. We try to apply median filter of the size of 7*7 in terms of renal size excluding those of pixels with zero. The results of the proposed ROI extraction are shown in Fig. 2(b). We can observe from Fig. 2 that the resultant image after noise removal is more clear then that of the original one (Fig. 2(a)) . The ROIs are more attractive compared to that of Tsagaan's method (Fig. 2(c)).

3 Kidney Segmentation

Now, we would begin to segment the right and left kidney from two extracted ROIs on each slice. We utilized a series of image processing techniques including region growing, labeling, filling and mathematical morphology such as erosion and dilation. In addition, we have modified those techniques to fulfill the segmentation requirement.

3.1 Adaptive Region Growing

There are three problems in the region growing process including initial seeds selection, similarity criterion of growing, and the formulation of termination criterion. To conquer these problems, we proposed the adaptive criteria for region growing by constructing a model of direction (see Fig. 3) in terms of five frequent locations of kidneys within ROIs. In this step, we search the right kidney related to directional sequence that is less different from that of left one. Besides, to enhance the learning effect, we choose an adaptive interval of threshold θ_1 that allows to be updated by each processing iteration or each direction is discontented with gray level criterion. The search operation will not be terminated until uniform mesh is found in all directions, meanwhile the threshold θ_1 will be also updated. Thus, we provide a more formal formulation of this approach.

- Initial seeds: A new initial search point is segmented in terms of renal trend in different slice, as

$$\begin{aligned} x^{'} &= x^{'}_{center} - \rho(a_i - a_0) \\ y^{'} &= y^{'}_{center} - \rho(a_i - a_0) \end{aligned} \quad (3)$$

$$\begin{aligned} x^{''} &= x^{''}_{center} + \rho(a_i - a_0) \\ y^{''} &= y^{''}_{center} - \rho(a_i - a_0) \end{aligned} \quad (4)$$

where ρ is a threshold (ρ=2.2), $x^{'}$, $y^{'}$, and x'', y'' are coordinates of left ROI and right ROI, respectively, ($x^{'}_{center}, y^{'}_{center}$) and ($x^{''}_{center}, y^{''}_{center}$) are the center points for those ROIs, a_i is an index of slice i being processed and a_0 is the index of starting slice in a dataset. Since the kidney is a homogeneous located inside the ROI, we constructed a model of direction where the search path is illustrated by d_4, d_1, d_5, d_3, and then d_2 in turn (shown in Fig. 3). We compute the difference between the maximum and minimum pixel values in a 7*7 mesh along a direction of d_i, if the value is lager than a threshold (20), it would be not suitable as an initial seed (i.e. non-homogeneous area). The search procedure lasts until an appropriate seed is found.

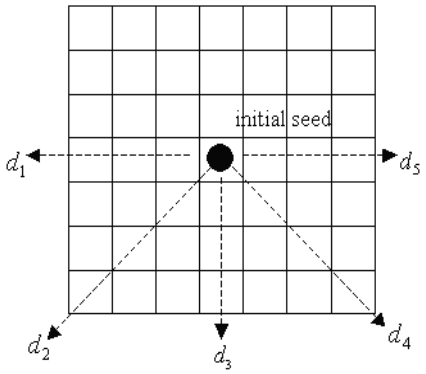

Figure 3: Direction finding for initial seed.

- Kidney growing criterion: Once the initial seed is located, we start to perform the region growing from this seed by the following equation:

$$\left|\Psi(i,j) - \Theta_{local}\right| \le t_0 \quad \forall (i,j) \subseteq R_{ROIs} \quad (5)$$

and

$$\Theta_{local} = (\Re_{\max} + \Re_{\min})/2 \quad (6)$$

where $\Psi(i,j)$ is a pixel which satisfies 8-connected condition for the initial seed, t_0 is a heuristic threshold, $\Re_{\max}$ and $\Re_{\min}$ denote

maximum and minimum of intensity in the mesh, respectively. According to the growing criterion, the growing would be terminated when $\Psi(i,j) - \Theta_{local} > t_0$.

3.2 Region Modification

Once the binary image has been obtained by the adaptive region growing, there are still trivial and irregular objects with concaves scattering in the candidate kidney region. For this, the region modification technique is essential to improve the segmentation accuracy under various conditions such as the contrast media injection time and rate, image intensity variations, and blood flow rate. We implemented the region modification by utilizing a series of image processing skills including: pixels filling, erosion, labeling, and dilation [9]. The details will be presented in this section. To identify those irregular objects, an efficient filling algorithm is proposed which is modified from the point containment technique[10]. Let R_1 and R_2 are two regions in one ROI in the binary images, namely, pixels in R1 are with gray level 0 and pixels in R2 are with gray level 255. Given a transformation represented for the following equation:

$$f^{'}(x,y) = \begin{cases} 1, if\ f(x,y) = 0, \forall (x,y) \in R_1 \\ 0, otherwise \end{cases} \quad (7)$$

where $f^{'}(x,y)$ is an inverse image of the binary image $f(x,y)$. Then we apply the region growing once again by selecting the pixels in the ROIs as the initial seeds. During the process of region growing, all pixels in R1 will be inverted and constituted the final image:

$$H(x,y) = F(x,y) + G(x,y)\ \forall x,y \in R_1, R_2 \quad (8)$$

where $H(x,y)$, $F(x, y)$, and $G(x,y)$ represent the resultant filled image, original binary image, and the image obtained from the second region growing, respectively. However, some problems may be found. For example, the threadlike region would belong to non-kidney. In addition, a bridge between two regions may also occur. We used the conventional erosion technique as the following equation to solve this problem.

$$A \ominus B \cap_{b \in B} (A)_{-b} \quad (9)$$

	1	1	1	
1	1	1	1	1
1	1	1	1	1
1	1	1	1	1
	1	1	1	

Figure 4: The designed structure element *B*.

where *A* denotes the current binary image, *B* denotes the structuring element, *b* denotes the individual elements of B, and -*b* denotes the inverse of *b*. The designed structuring element B (Fig. 4) is not as same as the common 3x3 mask. A circle structure element is applied instead. The result of this operation indulges region separation and retains more smooth object boundary. Once the erosion operation has been applied, the region will be separated into two or more sub-regions. It is indeed to apply a labeling approach to size up each sub-regions.

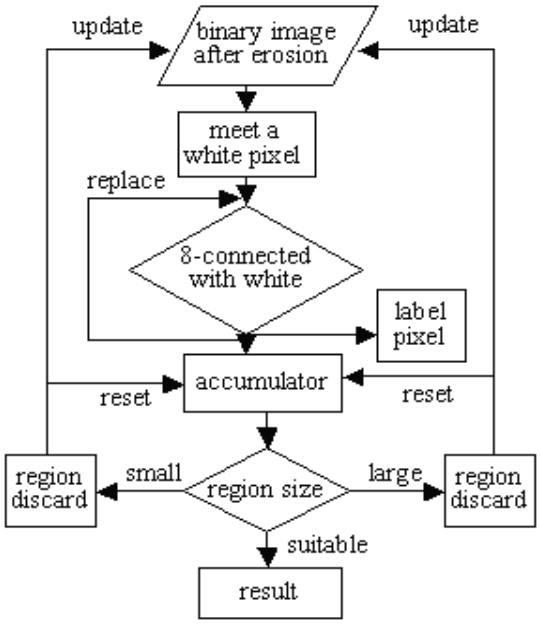

Figure 5: Labeling procedure of our method.

For this, we introduce a fine method to evaluate the region size directly by an accumulation and the recursive process illustrated in Fig. 5. Furthermore, it is necessary to apply the dilation operation to compensate for the above-mentioned erosive region. A formal definition of dilation is presented as below:

$$A \oplus B = \cup_{b \in B} (A)_b \quad (10)$$

where the definition of A, B, and b is same as those of erosion operation. The relationship between erosion and dilation can be understood by comparing their operation. Finally, we will display the segmentation image of kidney by pasting the resulting area of region growing and modification from the original CT images. The main consideration is that the precise location of kidneys display may change slice by slice or patient by patient on abdominal CT image.

3.3 Contour Visualization and Edge Detection

To provide better visualization for physicians on the CT image, the second-order neighborhood edge detection technique is applied to depict the contour of kidney on the abdominal CT images. The second order neighborhood is applied to distinguish the relationship between the current pixel (i,j) and its neighboring pixels $\hat{N}(i,j)$. An edge may pass through the second-order neighborhood of a pixel in one of the four various masks, namely horizontal, vertical, northeast diagonal, and northwest diagonal[7]. In Equations 11 and 12, the values of $HE(i,j)$, $VE(i,j)$, $NE(i,j)$ and $SE(i,j)$ as well as "*edge strength*" are induced by the horizontal, vertical, northeast diagonal, and northwest diagonal edge masks, respectively.

$$\begin{cases} HE(i,j) = | G(i,-1j+1) + 2G(i,j+1) \\ \qquad + G(i+1,j+1) - G(i-1,j-1) \\ \qquad - 2G(i,j-1) - G(i+1,j-1) | \\ VE(i,j) = | G(i+1,j-1) + 2G(i+1,j) \\ \qquad + G(i+1,j+1) - G(i-1,j-1) \\ \qquad - 2G(i-1,j) - G(i-1,j+1) | \end{cases} \tag{11}$$

$$\begin{cases} NE(i,j) = | G(i+1,j) + 2G(i+1,j+1) \\ \qquad + G(i,j+1) - G(i-1,j) \\ \qquad - 2G(i-1,j-1) - G(i,j-1) | \\ SE(i,j) = | G(i,j+1) + 2G(i-1,j+1) \\ \qquad + G(i-1,j) - G(i,j-1) \\ \qquad - 2G(i+1,j-1) - G(i+1,j) | \end{cases} \tag{12}$$

where $G(i+1,j+1)$ denotes the gray level of the pixel at the coordinate $(i+1,j+1)$. $ME(i,j)$ is defined as the maximum of four edge strengths for evaluating the "*local maximum edge strength*" of pixel (i,j),

$$ME(i,j) = max\{HE(i,j), VE(i,j), NE(i,j), SE(i,j)\} \tag{13}$$

The contour is formed by connecting pixels with $ME(i,j) \geqq 255$.

4 Experimental Results

The kidney CT data used in this study was obtained from three CT scanners including HiSpeed LX/i by GE, PQ2000 by PICKER, and Aquilion Multi 16 by TOSHIBA. Thirty cases of abdominal CT images sequence were collected in the dataset. Each case contains around 7 to 20 slices due to different cross-section thickness protocol of different CT scanners. One particular viewpoint of this research domain is that there is no precise ground rule of truth. Conventionally, most professional physicians make diagnosis on the CT slices directly by observation. They may make around 5 to 10 pixels width of mismatch by drawing the contours of complex regions in an image of size 512x512. In the worst case, there will be even more than 10 pixels width mismatch [6]. In the proposed segmentation system, we evaluated the performance objectively by the attending physicians. Moreover, the evaluation was made based on the accuracy of the outermost contours only. The segmentation result on each slice is graded as "*G*"(Good), "*A*"(Acceptable) or "*B*"(Bad), namely, "*G*" denotes the CAD system is comparable to surgical work and the width of mismatch is less than 15 pixel, "*A*" denotes the result is worse than "G", however the correct segmented kidney region or under- segmentation region is at least 75 percentage overlapped with the entire true area. "*B*" denotes the detected kidney region is smaller than 75% of the true area. The proposed system was examined on 291 images with better image quality (B.Q.) from 20 patients and examined on 90 testing images with poor quality (P.Q) from 10 patients. The result of computer-aided segmentation of half of the data (10 B.Q. and 5 P.Q) was graded by the author, and the other was graded by two physicians. We concluded the examination results in Table 1 and Table 2. In Table 1, the evaluation of the system performance by the author achieves to 94.95% correct segmentation above the grade "*G*" and "*A*". The ratio of poor segmentation is as low as 5.5%. Table 2 shows the evaluation from two professional physicians. Since the criteria of physicians is more restrict and conservative, the segmentation performance is not as good as that evaluate by the author (70.3% v.s. 82.55% in grade "*G*", 27.1% v.s. 13.7% in grade "*A*"). Nevertheless, the evaluation of the part of "*B*" grade is much less than that of author. In other words, physicians agree that the proposed system can maintain the

segmentation quality above certain level. Judging by comparing Figure 2(b) and (c), we learn that our technique emphasizes the relaxation of ROIs setting better than that of Tsagaan [1], et. al. whose ROIs are fixed. Besides, the performance has been improved by considering the relation of 3D structure of consecutive slices. From the above-mentioned statistics, the performance evaluations show a satisfactory segmentation result.

Grade	Left kidney		Right kidney		Average
	B.Q.	P.Q.	B.Q.	P.Q.	
"G"	85.3%	86.1%	80.3%	78.5%	82.55%
"A"	10.5%	11.9%	13.8%	18.6%	13.7%
"B"	4.2%	2%	5.9%	2.9%	3.75%

Table 1: Performance evaluation by author: 10 B.Q. and 5 P.Q cases.

Grade	Left kidney		Right kidney		Average
	B.Q.	P.Q.	B.Q.	P.Q.	
"G"	69.3%	70.1%	70.3%	71.5%	70.3%
"A"	27.5%	26.5%	27.8%	26.6%	27.1%
"B"	3.2%	3.4%	1.9%	1.9%	2.6%

Table 2: Performance evaluation by physicians: 10 B.Q and 5 P.Q. cases.

5 Conclusions

In this paper, an efficient method for kidney segmentation on abdominal CT images has been proposed systematically. The kidney ROIs is first obtained based on a priori anatomical knowledge of kidney. Furthermore, mean and conditional median filtering are integrated to perform preliminary noise removal. Such a flexible ROIs extraction scheme as we introduced should be very attractive for various kidney location appeared on abdominal CT image. Next, we develop an adaptive region growing for kidney segmentation and provide a strategy of region modification for the consideration of accurate extraction. For supplying user with better visualization, the concept of second-order neighborhood is used for edge extraction.

References

[1] B. Tsagaan, A. Shimizu, H. Kobatake and K. Miyakawa, 2002, "An Automated Segmentation Method of Kidney Using Statistical Information", *Proceedings of Medical Image Computing and Computer Assisted Intervention, 1*, 556-563.

[2] R. Pohle and K. D. Toennies, 2001, "A New Approach for Model-Based Adaptive Region Growing in Medical Image Analysis", *9th International Conference on Computer Analysis of Images and Patterns, 2124,* 238-246.

[3] R. Pohle and K. D. Toennies, 2001, "Segmentation of Medical Images using Adaptive Region Growing", *Proceedings of SPIE, 4322*, 1337-1346.

[4] R. Pohle and K. D. Toennies, 2001, "Self-Learning Model-Based Segmentation of Medical Images", *Image Processing and Communications, 7*, 97-113.

[5] X. Wang, L. He, C. Y. Han and W. G. Wee, 2002, "Deformable Contour Method: A Constrained Optimization Approach", *British Machine Vision Conference*, 183-192.

[6] M. Kobashi and L. G. Shapiro, 1995, "Knowledge-Based Organ Identification from CT Images", *Pattern Recognition, 28*, 475-491.

[7] J. Fan, D. K. Y. Yau, A. K. Elmagarmid and W. G. Aref, 2001, "Automatic Image Segmentation by Integrating Color-Edge Extraction and Seeded Region Growing", *IEEE Transactions on Image Processing, 10*, 1454-1466.

[8] S. H. Kim, S. W. Yoo, S. J. Kim, J. C. Kim and J. W. Park, 2000, "Segmentation of Kidney without using Contrast Medium on Abdominal CT Image", *5th International Conference on Signal Processing, 2*, 1147-1152.

[9] J. S. Hong, T. Kaneko, S. Sekiguchi and K. H. Park, 2001, "Automatic Liver Tumor Detection from CT", *IEICE Transactions on Information and System, E84-D*, 741-748.

[10] A. E. Fabris, L. Silva and A. R. Forrest, 1997, "An Efficient Algorithm for Non-simple Closed Curves using the Point Containment Paradigm", *SIBGRAPI'97,* http:// mirror.impa.br/sibgrapi97/ anais/pdf/art17.pdf.

[11] R. C. Gonzalez and R. E. Woods. 2002, "Digital Image Processing", *Addision-Wesley*, 2nd edition.

[12] J. Z. Chen, G. S. Tracton, M. Rao, S. Joshi, E. L. Chaney and S. M. Pizer 2002, "Comparison of Automatic and Human Segmentation of Kidneys from CT Images", *International Journal of Radiation Oncology*Biology*Physics, 54*, 82.